Open access • Journal Article • DOI:10.1016/S0166-1280(03)00152-0

Excited state geometries within time-dependent and restricted open-shell density functional theories — Source link

Michael Odelius, Dimitri N. Laikov, Jürg Hutter

Institutions: University of Zurich

Published on: 25 Jul 2003 - Journal of Molecular Structure-theochem (Elsevier)

Topics: Orbital-free density functional theory, Hybrid functional, Excited state, Time-dependent density functional theory and Density functional theory

Excited state geometries within time-dependent and restricted open-shell density functional theories

Odelius, M; Laikov, D; Hutter, J

Excited state geometries within time-dependent and restricted open-shell density functional theories

Abstract

Singlet excited state geometries of a set of medium sized molecules with different characteristic lowest excitations are studied. Geometry optimizations of excited states are performed with two closely related restricted open-shell Kohn-Sham methods and within linear response to time-dependent density functional theory. The results are compared to wave-function based methods. Excitation energies (vertical and adiabatic) calculated from the open-shell methods show systematic errors depending on the type of excitation. However, for all states accessible by the restricted methods a good agreement for the geometries with time-dependent density functional theory and wave-function based methods is found. An analysis of the energy with respect to the mixing angle for the singly occupied orbitals reveals that some states (mostly {[}n --> pi{*}]) are stable when symmetry constraints are relaxed and others (mostly [pi --> pi{*}]) are instable. This has major implications on the applicability of the restricted open-shell methods in molecular dynamics simulations.

Excited State Geometries within Time–Dependent and Restricted Open–Shell Density Functional Theories

Michael Odelius [a] Dimitri Laikov [b] Jürg Hutter [a,*]

[a] *Institute of Physical Chemistry, University of Zürich, Winterthurerstr. 190, CH-8057 Zürich, Switzerland*

[b] *Institute of Organic Chemistry, University of Zürich, Winterthurerstr. 190, CH-8057 Zürich, Switzerland*

Abstract

Singlet excited state geometries of a set of medium sized molecules with different characteristic lowest excitations are studied. Geometry optimizations of excited states are performed with two closely related restricted open-shell Kohn–Sham methods and within linear response to time-dependent density functional theory. The results are compared to wave-function based methods. Excitation energies (vertical and adiabatic) calculated from the open–shell methods show systematic errors depending on the type of excitation. However, for all states accessible by the restricted methods a good agreement for the geometries with TDDFT and wave-function based methods is found. An analysis of the energy with respect to the mixing angle for the singly occupied orbitals reveals that some states (mostly $[n \rightarrow \pi^*]$) are stable when symmetry constraints are relaxed and others (mostly $[\pi \rightarrow \pi^*]$) are instable. This has major implications on the applicability of the restricted open–shell methods in molecular dynamics simulations.

1 Introduction

In the last decade first–principles molecular dynamics (MD) emerged as a powerful tool to study properties of materials and mechanisms in chemical

* Corresponding author.
Email address: hutter@pci.unizh.ch (Jürg Hutter).

[1] We like to thank B. O. Roos for sharing CASPT2 results for pyrrole, and I. Frank for stimulating discussions. This work was supported in part by the Swiss National Science Foundation (Nr. 21-63305.00)

reactions. [1,2] Because those simulations are computationally very demanding most of the calculations are performed within density functional theory (DFT). An extension of these techniques to electronically excited states would significantly extend the field of applications. Currently, most dynamical studies of photo–chemical reactions are limited to pre–calculated surfaces, including only a few degrees of freedom.

Many photochemical applications and state-of-the art femto–second laser experiments involve chromophores in condensed systems, such as solid matrices and liquid solutions [4]. The combination of an on–the–fly calculation of the excited state surface with molecular dynamics techniques will allow to include much more degrees of freedom into the calculation, especially simulations of photo–chemical reactions in explicit solvents will be possible. However, to be of general interest, the electronic structure calculations have not only to be accurate but also simple enough to allow for computationally efficient combination with molecular dynamics.

Several advanced and computationally highly demanding methods have been developed for a proper description of excited states. Many excited states have intrinsically a multi-configurational character, and the methods, which are generally accepted to give accurate results are constructed to this means. Multi–reference configuration interaction (MRCI) [5], perturbation theory combined with complete active space methods (CASPT2) [6,7] and equation–of–motion coupled cluster theory (EOM-CC) [8] are the methods of choice to calculate excited state surfaces and excitation energies. However, for the purpose of *ab initio* molecular dynamics (MD) simulations, it is necessary to employ computationally less demanding theoretical tools. In the framework of Car-Parrinello dynamics [1–3], the restricted open-shell Kohn-Sham (ROKS) method [9] was developed. The method has been used to study excited state dynamics in gas phase and condensed systems [9–11]. Recently the methods was combined with non–adiabatic dynamics to study photo chemical processes [12]. A more general version of the method was derived at the same time by another group [13,14]. In this work we also consider the restricted open-shell singlet (ROSS) method [15,16], which is very closely related to the ROKS method. We make comparisons to linear response calculations within time-dependent density functional theory (TDDFT) [17,18], which is used as a reference DFT method and a possible candidate for studying excited state dynamics for large systems with *ab initio* MD simulations. The TDDFT has proven its usefulness in the calculation of electronic spectra from vertical excitations, but there are few studies of excited state potential surfaces [17–19].

For the use of the ROKS/ROSS or TDDFT methods in the study of excited state dynamics of molecules in gas phase and condensed matter, it is essential to know if the methods capture the correct lowest excited state and how well they describe the excited state potential. In the following we will examine

both the quality of the description and the limitations of the methods. To this end, we have selected a set of organic molecules with different types of lowest excited singlet states, and calculated the vertical excitations energies and excited state geometries.

Since we have not made an extensive comparison of different functionals, the present study is an assessment both of the different methods and the functional of choice (BLYP). An extension to hybrid functionals would be particularly interesting, since they are known to often give a more accurate description of excitation energies. However, for computational reasons the plane-wave basis is not suited for evaluating the exact exchange in the hybrid functionals. Thus, the possibly improved accuracy would come at the expense of computational efficiency crucial for the use in ab initio MD simulations.

2 Methods

The methods employed in this study are described in detail elsewhere [2,9,15,19]. Therefore we will only give a brief description of the most important features. The restricted open-shell Kohn-Sham (ROKS) method can be derived using an ensemble DFT or from the empirical, although well established sum rule of DFT [9,13,14,20,21]. For the first excited singlet state, the ROKS method can be described as follows. Promoting one electron from the highest occupied molecular orbital (HOMO) into the lowest unoccupied molecular orbital (LUMO) in a closed–shell system with 2n electrons assigned to n doubly occupied orbitals leads to four different one–determinantal wavefunctions. Two of these correspond to energetically degenerate triplet states (t), whereas the other two are mixed states (m) and not eigenfunctions of the total spin operator. Spin densities derived from these determinants are denoted by $n_{\mathrm{m}}^{\alpha}, n_{\mathrm{m}}^{\beta}, n_{\mathrm{t}}^{\alpha}, n_{\mathrm{t}}^{\beta}$, and add up to a total excited state density

$$n(\mathbf{r}) = n_{\mathrm{m}}^{\alpha}(\mathbf{r}) + n_{\mathrm{m}}^{\beta}(\mathbf{r}) = n_{\mathrm{t}}^{\alpha}(\mathbf{r}) + n_{\mathrm{t}}^{\beta}(\mathbf{r}) \tag{1}$$

The total energy of the singlet state is calculated in the ROKS method as

$$E_{\mathrm{S}_1}[\{\Phi_i\}] = 2E_{\mathrm{m}}^{\mathrm{KS}}[\{\Phi_i\}] - E_{\mathrm{t}}^{\mathrm{KS}}[\{\Phi_i\}] \tag{2}$$

where $E_{\mathrm{m}}^{\mathrm{KS}}$ and $E_{\mathrm{t}}^{\mathrm{KS}}$ are the Kohn–Sham energies of the mixed and triplet determinants respectively. E_{S_1} is a functional of the orbitals Φ_i

$$E_{\mathrm{S}_1}[\{\Phi_i\}] = T_{\mathrm{s}}[\{\Phi_i\}] + E_{\mathrm{ext}}[n] + E_{\mathrm{H}}[n] + 2E_{\mathrm{xc}}[n_{\mathrm{m}}^{\alpha}, n_{\mathrm{m}}^{\beta}] - E_{\mathrm{xc}}[n_{\mathrm{t}}^{\alpha}, n_{\mathrm{t}}^{\beta}] \tag{3}$$

and is minimized under the constraint

$$\langle \Phi_i \mid \Phi_j \rangle = \delta_{ij}. \tag{4}$$

In the ROSS method a slightly different approach is used and the energy difference between the singlet, mixed and triplet states is calculated using the exchange integral
$K = \langle \Phi_a \Phi_b \mid \Phi_a \Phi_b \rangle$ of the singly occupied orbitals. The final energy expression used is

$$E_{\mathrm{S_1}}[\{\Phi_i\}] = T_{\mathrm{s}}[\{\Phi_i\}] + E_{\mathrm{ext}}[n] + E_{\mathrm{H}}[n] + E_{\mathrm{x}}[n_{\mathrm{t}}^{\alpha}, n_{\mathrm{t}}^{\beta}] + 2K + E_{\mathrm{c}}[n_{\mathrm{m}}^{\alpha}, n_{\mathrm{m}}^{\beta}] \tag{5}$$

This expression is minimized subject to the orthogonality constraint in Eq. 4. For both methods, ROKS and ROSS, the orbitals are calculated variationally and the determination of gradients with respect to nuclear degrees of freedom, as needed in geometry optimizations and molecular dynamics simulations is straightforward.

The calculation of excitation energies within time–dependent DFT makes use of linear response theory [19]. It has been used extensively in recent years for the study of vertical exciation energies. However, the non-variational character of this method complicates the calculation of nuclear gradients and makes their implementation a non trivial task [22,23,34].

3 Computational Details

A major part of the DFT (both ground state and excited state; ROKS and ROSS) calculations were performed with a Car-Parrinello MD simulation program [27] based on a plane wave basis for the electronic wave-functions combined with a pseudopotential description. The performance of both excited state methods with respect to computational efficiency is comparable. The additional exchange integral in the ROSS method is calculated in Fourier space

$$K = \langle \Phi_{\mathrm{a}} \Phi_{\mathrm{b}} \mid \Phi_{\mathrm{a}} \Phi_{\mathrm{b}} \rangle = 4\pi \sum_{G \neq 0} \frac{\rho_{\mathrm{ab}}(-G)\rho_{\mathrm{ab}}(G)}{G^2}, \tag{6}$$

and the overlap density $\rho_{\mathrm{ab}}(r) = \Phi\mathrm{a}(r)\Phi_{\mathrm{b}}(r)$ on the real space grid. We used norm-conserving pseudopotentials, expressed in the Kleinman-Bylander form [28], with a 70 Ry kinetic energy cut-off for the plane wave expansion for the Kohn-Sham wave-functions. For hydrogen a local pseudopotential parameterized with one Gaussian was used [29]. The pseudopotentials for carbon,

nitrogen and oxygen were of Martin-Troullier type [30] and were non-local in the $l = 0$ channel. In the pseudopotential generation, the cut-off radii was set to 1.23 a.u.(C), 1.12 a.u.(N) and 1.05 a.u.(O) for both the s and p channels. The ground state was described using the B-LYP functional [31,32]. To enable the study of isolated systems, the inherent periodicity in the plane-wave calculations was avoided solving Poisson's equation for non-periodic boundary conditions [33]. Cell sizes of 15x15x10 Å were used in the calculations, which was sufficient to converge the energies and geometries with respect to the cell parameters. The restricted open-shell Kohn-Sham (ROKS) [9] and the restricted open-shell singlet (ROSS) [15,16] calculations were carried out within the same theoretical framework as the ground state.

The geometry optimizations with the TDDFT method were performed with a DFT program using Gaussian basis sets[34], in which the electron density is fitted to an auxiliary basis set. The fitted density is used in the calculation of the Coulomb energy and the exchange and correlation functionals. The Gaussian basis sets used in this study are of triple-zeta quality and of segmented contraction scheme of the size (5s1p)/[3s1p] for H, (11s6p2d)/[6s3p2d] for C, N, O, and (15s11p2d)/[10s6p2d] for S, the corresponding auxiliary basis sets consist of uncontracted Gaussian functions and are of the size (5s2p) for H, (10s3p3d1f) for C, N, O, and (14s3p3d1f1g) for S. These basis sets have been derived along similar lines as in the TZV work of the Karlsruhe group [35,36], but with an additional constraint of shared exponents for all angular momenta, which allows 3-4 times faster evaluation of the required Coulomb-type integrals. The numerical accuracy of our density-fitting procedure for ground state DFT calculations is well documented [37], and the advantage of using auxiliary basis sets in TDDFT calculations has been demonstrated [38]. The accuracy of the auxiliary basis set was checked by comparing TDDFT excitation energies to values calculated with the Gaussian 98 program.

In addition we also implemented the ROKS method into the Gaussian based DFT program[34]. This allowed us to check the accuracy of basis sets and pseudopotentials used in the programs.

4 Test Calculations

By examining the character of the first excited state for vertical excitations at the ground state geometry, we can determine if the ROKS/ROSS methods give a correct ordering for the lowest excited state. The order of the states within TDDFT for this set of molecules has previously been thoroughly studied [19,39]. The TDDFT method performs well in most cases for the lowest excitations, with errors in the order of a few tenth of eV. Rydberg states are systematically too low in energy (by as much as a few eV) due to the wrong

asymptotic behavior in most current DFT functionals [39]. If the erroneous long-distance decay is corrected, the TDDFT method gives errors for Rydberg states which are smaller than those for valance excitations, but exaggerating valence-Rydberg state mixing [39].

The ROKS and ROSS methods allow only for the first excited singlet state to be calculated. However, in symmetric molecules additional states can be accessed, since the lowest excited singlet state in each irreducible representation can be studied. This technique was used whenever applicable to investigate higher excited states with these methods.

For each molecule, the quality of the B-LYP functional was assessed by comparing the ground state geometry to Møller-Plesset perturbation (MP2) calculations. MP2 [40], CIS and B-LYP DFT calculations were performed with the Gaussian 98 [41] program using a 6-311G(2d,p) basis set. In the CIS calculations diffuse functions [6-311++G(2d,p)] were added to ensure a reliable description of the excited states.

Vertical excitation energies were calculated at the optimized ground state geometries. For the CIS method, the Hartree-Fock geometry was used and for the ROKS/ROSS and TDDFT calculations, we used geometries obtained with the same functional and basis set. The agreement in bond lengths between the MP2 and the density functional B-LYP calculations was within 1 % and for the bond angles the agreement was within half a degree. The difference between the pseudopotential plane wave calculations and the Gaussian basis set calculations was generally negligible, except for thiophene in which the carbon-sulphur bond is underestimated by almost 1 % in the pseudopotential treatment.

4.1 Excited states ordering

As the restricted open–shell methods require that the singly occupied orbitals in the calculation belong to different irreducible representations some of the excited states were not accessible by these methods. For thiophene, the lowest excited state is of A_1 symmetry, and involves a transition bewteen orbitals of the same symmetry. For the same reason, the optimized excited state geometry of pyridine had to be restricted to C_{2v} symmetry.

Vertical excitations from the optimized ground state geometries were examined to assess the nature of the S_1 state in the ROKS/ROSS methods. The ordering of the lowest states with ROSS was correct for all molecules considered except for cyclo–pentadiene, whereas for ROKS the $[\pi \rightarrow \pi^*]$ excitation is lower than the Rydberg state in furan. The ROKS method generally underestimates the excitation energies. Excitation energies for Rydberg states

Table 1. Vertical excitation energies for the lowest excitations. For the ROKS method, results from calculations with Gaussian type basis sets are presented within parenthesis. [a] from references [52,23] and references therein. [b] Reference [39] and references therein. [c] Reference [46]. [d] Reference [43]. [e] TDDFT (B-LYP) and CASPT2 results from Reference [44].

Molecule	Type	CIS	ROSS	ROKS	TDDFT	CASPT2	EXP
Formaldehyde	$A_2[n \rightarrow \pi^*]$	4.74	3.71	3.50(3.70)	3.86	3.91[a]	4.07[a]
s-Tetrazine	$B_{3u}[n \rightarrow \pi^*]$	3.48	2.09	1.72	1.92(1.90[b])	1.96[bc]	2.25[b]
Pyridine	$B_1[n \rightarrow \pi^*]$	6.26	4.59	4.37	4.37(4.76[d],4.39[e])	5.00[e]	4.59[e]
	$A_2[n \rightarrow \pi^*]$	6.89	-	(4.96)	4.48(5.07[d],4.44[e])	5.25[e]	5.43[e]
	$B_2[\pi \rightarrow \pi^*]$	6.25	-	(5.04)	5.26(5.47[d],5.29[e])	4.89[e]	4.99[e]
C-pentadiene	$B_2[\pi \rightarrow \pi^*]$	5.75	5.56	4.37	4.84(5.02[b])	5.27[b]	5.26[b]
	$A_2[\pi \rightarrow 3s]$	-	5.15	5.14	- (5.54[b])	5.65[b]	5.68[b]
Thiophene	$A_1[\pi \rightarrow \pi^*]$	6.77	-	-	5.48(5.64[b])	5.33[b]	5.33[b]
	$B_2[\pi \rightarrow \pi^*]$	6.28	6.11	5.46	5.48(5.65[b])	5.72[b]	5.64[b]
Furan	$A_2[\pi \rightarrow 3s]$	6.22	5.63	5.61	5.76(5.93[b])	5.92[b]	5.94[b]
	$B_2[\pi \rightarrow \pi^*]$	6.65	6.28	5.24	5.96(6.08[b])	6.04[b]	6.06[b]
Pyrrole	$A_2[\pi \rightarrow 3s]$	5.52	4.83	4.82(5.16)	4.66(5.05[b])	5.08[b]	5.22[b]
	$B_2[\pi \rightarrow \pi^*]$	6.58	6.04	5.38(5.50)	6.19(6.01[b])	6.00[b]	5.98[b]

Table 2
Adiabatic excitation energies for the lowest excitations (eV). For the ROKS method, results from calculations with Gaussian type basis sets are presented within parenthesis. [a] TDDFT, MRDCI and experimental results from Reference [23] and references therein. [b] CASPT2 and experimental results from Reference [46] and references therein. [c] TDDFT (B-LYP) , Equation-of-motion coupled cluster and experimental results from Reference [44] and references therein. [d] Equation-of-motion coupled cluster results from Reference [47]. [e] Equation-of-motion coupled cluster results and experimental data from Reference [48] and references therein.

Molecule		CIS	ROSS	ROKS	TDDFT	LITT	EXP
Formaldehyde		4.54	3.33	3.15(3.34)	3.50(3.48[a])	3.5[a]	3.5[a]
s-Tetrazine		3.33	1.96	1.60	1.79	1.79[b]	2.25[b]
Pyridine		5.57	4.17	3.99	3.99 (3.96[c])	4.80[c]	4.47[c]
	A_2	6.69	-	(4.24)	3.82 (3.74[c])	4.84[c]	-
	B_2	-	-	(4.82)	5.09 (5.10[c])	5.11[c]	4.90[c]
Cyclo-pentadiene		4.83	5.08	3.85	4.32	-	-
	A_2	-	4.98	4.98	-	-	-
Thiophene		-	-	-	-	-	-
	B_2	5.49	5.08	4.31	4.77	-	-
Furan	A_2	5.96	5.47	5.45	5.62	5.89[e]	5.91[e]
	B_2	5.96	5.71	4.71	5.30	-	-
Pyrrole		5.18	4.60	4.59	-	4.85[d]	-
B_2		6.22	5.50	4.74	-	-	-

are nearly identical in the two methods. The ROSS method is giving slightly higher excitation energies for $[n \rightarrow \pi^*]$ transitions, and considerably higher for $[\pi \rightarrow \pi^*]$ transitions.

Furan has a lowest excited state of A_2 Rydberg type, usually denoted $[\pi \rightarrow 3s]$ or $[\pi \rightarrow \sigma^*]$, and the $[\pi \rightarrow \pi^*]$ valence transition is the S_2 state. In pyrrole, which has an A_2 Rydberg S_1 state, there are several Rydberg and an A_1 valence state with lower excitation energies than the B_2 $[\pi \rightarrow \pi^*]$ valence transition. It is known that Rydberg states are very sensitive to the box size in periodic calculations [42]. In an attempt to see if the ROKS method could give the correct Rydberg type S_1 state for furan, we increased the cell parameters to 24 Å and performed ROKS calculations and determined the lowest unoccupied states in the ground state Kohn–Sham calculation. Despite the large effect of the cell size on the unoccupied energy levels, the S_1 state of the ROKS method was unaffected.

4.2 Adiabatic energies

In order to understand how well the different methods describe the excited state potentials, we turn to a comparison of excited state geometries. The adiabatic excitation energies, contained in Table 2, again show that the ROKS method underestimates all excitation energies, in particular for $[\pi \rightarrow \pi^*]$ transitions. ROSS gives identical results for the Rydberg excitations, but $[n \rightarrow \pi^*]$ and especially $[\pi \rightarrow \pi^*]$ excitations are improved. The first excited singlet state of all the molecules studied possess at least C_s symmetry which enabled us to determine reliable results for ROKS/ROSS. However, for pyridine it was only possible to study the excited state at planar geometries.

There exists only a few studies of excited state geometries within TDDFT [22–25]. In addition, we studied the same systems with the singly-excited configuration interaction (CIS) method. The CIS method is in widespread use. However, it is known to give an insufficient description in many applications [26], and we include the comparison to show that the ROKS/ROSS, and TDDFT methods are generally superior to the CIS method, with a smaller and comparable computational effort, respectively. Accurate excited state geometries are not easily accessible in experiment. Therefore we would have liked to compare our results with reference calculations employing more advanced methods. For a few of the molecules, higher level calculations can be found in the literature. Whenever possible we used this data to evaluate the ROKS, the ROSS and the TDDFT methods, but for all other cases we are limited to an internal comparison between the DFT methods.

5 Results

5.1 Formaldehyde, s-Tetrazine, and Pyridine

Molecules with $[n \rightarrow \pi^*]$ transitions were already examined in the original ROKS work [9] showing that the ROKS method gives a good description of the geometries in the lowest excited singlet state. In this work, we further studied $[n \rightarrow \pi^*]$ excitations in molecules with aromatic π systems. We included also formaldehyde, which has been treated previously by the ROKS [9] and TDDFT methods [23]. In formaldehyde and s-tetrazine, the lowest singlet excitation occurs from the highest occupied orbital (HOMO) into the lowest unoccupied orbital (LUMO), and it is energetically well separated from the other singlet states. In s-tetrazine, there are several close lying occupied n and unoccupied π^* orbitals, which could complicate the description of the excitation. In pyridine, another molecule studied in this class there are several

Table 3
First excited singlet state geometries of formaldehyde (Å /degrees) τ: oxygen out-of-plane angle. For the ROKS method, the results from the calculations with a Gaussian type basis are presented within parenthesis. [a] from reference [23] and references therein.

	CIS	ROSS	ROKS	TDDFT	MRCI[a]	EXP[a]
r_{CO}	1.246	1.340	1.329(1.319)	1.320(1.317[a])	1.334	1.323
r_{HC}	1.087	1.098	1.101(1.106)	1.100(1.102[a])	1.116	1.098
Δ_{HCH}	117.8	117.7	116.0(114.1)	117.2(117.1[a])	120.2	118.4
τ	23.2	33.5	36.4 (39.1)	33.8(33.0[a])	34.5	34.0

Table 4
First excited singlet state geometries of s-tetrazine (D_{2h} symmetry); the same notation as in table 3 is used. [a] from Reference [46] and references therein.

	CIS	ROSS	ROKS	TDDFT	CASPT2[a]	EXP[a]
r_{NN}	1.284	1.331	1.332	1.334	1.320	1.349
r_{CN}	1.313	1.341	1.340	1.341	1.333	1.324
r_{CH}	1.069	1.084	1.084	1.086	1.073	-
Δ_{NCN}	119.8	121.2	121.3	121.2	121.5	123.2

close lying excited states arising from $[n \rightarrow \pi^*]$ and $[\pi \rightarrow \pi^*]$ transitions. The lowest excited singlet state in all three molecules result from an excitation of a lone-pair orbital of σ symmetry to a π^* orbital. In Tables 3, 4 and 5, the geometries of S_1 states obtained with different methods are compared.

In formaldehyde the elongation of the carbonyl bond seen experimentally is reproduced by the ROKS/ROSS and TDDFT methods (see Table 3). Formaldehyde bends upon excitation, and the bending angle is rather sensitive to the basis set, as can be seen in the difference between the plane wave and the Gaussian basis ROKS calculations.

The first excited state of s-tetrazine recieved recently much attention in the literature [46,53–55], and several high level calculations are available. The minimum structure within CIS and CASSCF has a reduced symmetry and bond lengths change significantly with respect to the ground state. CASPT2 calculations result in a geometry with D_{2h} symmetry, slight changes in bond length and only significant changes in bond angles. As seen in Table 4, all density functional based method are in good agreement with the CASPT2 geometry.

In pyridine, the vertical excitation spectrum from TDDFT was previously found to be in agreement with experiment [43,44]. As explained before the ROSS/ROKS had to be restricted to C_{2v} symmetry. Comparing the geome-

Table 5
First excited singlet state geometries of pyridine; the same notation as in table 3 is used. [a] Equation-of-motion coupled cluster results from Reference [44].

	CIS	ROSS	ROKS	TDDFT	EOM-CC[a]
SYM	C_s	C_{2v}	C_{2v}	C_s	C_s
r_{N1C2}	1.355	1.368	1.371	1.355	1.371
r_{C2C4}	1.371	1.381	1.382	1.383	1.389
r_{C4C6}	1.400	1.436	1.433	1.446	1.433
r_{C2H}	1.071	1.083	1.083	1.086	-
r_{C4H}	1.075	1.087	1.087	1.086	-
r_{C6H}	1.072	1.083	1.083	1.084	-
Δ_{CNC}	125.8	129.0	128.5	128.4	127
Δ_{NCC}	112.3	115.5	115.5	116.6	114
Δ_{C2C4C6}	120.0	120.7	120.9	119.8	120
Δ_{C4C6C5}	119.3	118.6	118.6	118.3	119
Δ_{NCH}	121.4	119.6	119.7	118.8	-
Δ_{C2C4H}	118.7	117.2	117.0	117.9	-
Δ_{C4C6H}	120.0	120.7	120.7	120.7	-
τ_{NCC}	34.0	0.0	0.0	6.5	27.1
τ_{CCC6}	7.1	0.0	0.0	4.5	9.0

tries from the ROSS/ROKS methods to that of the TDDFT method in Table 5, we see that the ROKS and TDDFT methods result in slightly different geometries around the nitrogen atom. All methods except CIS predict a lengthening on the carbon nitrogen bonds and the C_4C_6 bond and a shortening of the C_2C_4 bond. Bond angles are predicted by all methods within a few degrees whereas the ring puckering is much less pronounced in TDDFT than in the wavefunction based methods. No ring puckering could occur for the ROSS/ROKS methods due to the symmetry constraint. Additional calculations with CASSCF (8 electrons in 14 orbitals) using the MOLCAS [56] program resulted in a geometry similar to the TDDFT results. Finally, the equations-of-motion coupled cluster results [44] are for the bond length closer to the results from the ROKS method than to TDDFT. The S_1 state of pyridine has quite a large charge-transfer component, the dipole moment reduces from 2.3 D to 0.4 D upon vertical excitation. This could be a source for problems with the TDDFT.

Table 6. The lowest three singlet excited states of pyridine optimized in C_{2v} symmetry; the same notation as in table 3 is used. [a] Equation-of-motion coupled cluster results from Reference [44]

	ROKS			TDDFT			EOM-CC[a]		
	B_1	A_2	B_2	B_1	A_2	B_2	B_1	A_2	B_2
r_{N1C2}	(1.368)	(1.310)	(1.385)	1.355	1.319	1.383	1.369	1.313	1.380
r_{C2C4}	(1.385)	(1.489)	(1.432)	1.382	1.476	1.435	1.387	1.478	1.438
r_{C4C6}	(1.433)	(1.393)	(1.431)	1.447	1.396	1.433	1.434	1.400	1.437
r_{C2H}	(1.085)	(1.085)	(1.091)	1.086	1.083	1.089	-	-	-
r_{C4H}	(1.089)	(1.085)	(1.089)	1.086	1.083	1.088	-	-	-
r_{C6H}	(1.085)	(1.093)	(1.082)	1.083	1.091	1.083	-	-	-
Δ_{CNC}	(128.3)	(134.1)	(111.4)	128.5	133.3	113.5	129	136	113
Δ_{NCC}	(115.9)	(113.9)	(126.3)	116.6	114.1	125.4	115	113	126
Δ_{C2C4C6}	(120.7)	(117.0)	(121.4)	119.9	117.6	120.2	121	117	120
Δ_{C4C6C5}	(118.6)	(124.1)	(113.2)	118.3	123.4	115.3	119	124	115
Δ_{NCH}	(119.6)	(121.7)	(115.6)	118.6	120.0	115.3	-	-	-
Δ_{C2C4H}	(117.2)	(118.1)	(117.7)	117.9	118.6	118.7	-	-	-
Δ_{C4C6H}	(120.7)	(118.0)	(123.4)	120.8	118.3	122.4	-	-	-

By constraining the geometry optimization to C_{2v} symmetry, we determined the geometries of the lowest excited B_1 $[n \rightarrow \pi^*]$ state and of the S_2 A_2 $[n \rightarrow \pi^*]$ and S_3 B_2 state $[\pi \rightarrow \pi^*]$ states (see Table 6). The ROKS/ROSS calculations result in geometries very close to the EOM-CC results.

We can summarize that for both, formaldehyde, and s-tetrazine the ROKS and TDDFT methods results are in close agreement with each other and with experiment, whereas the CIS method clearly fails to describe the potential energy surfaces. For formaldehyde, s-tetrazine and pyridine, for which there exist studies with more advanced computational methods and experimental data is available, we can definitely state that TDDFT performs very well. The same observation holds for all states accessible by the ROSS/ROKS methods (See Tables 5 and 6).

5.2 Cyclo-Pentadiene, Thiophene, Furan, and Pyrrole

The vertical excitations of the set of 5-membered rings have previously been studied with TDDFT, coupled cluster techniques, and CASPT2 [39,47,48]. In the present study some of the vertical excitation energies differ from those in the literature [39,43], since different basis sets and functionals and no asymptotic corrections were used. In all molecules the conjugated π system is involved in a set of low energy valence excitations, which overlap with low lying Rydberg states. The S_1 $[\pi \rightarrow \pi^*]$ state in cyclo-pentadiene is a HOMO to LUMO transition of B_2 symmetry. In thiophene, an valence $[\pi \rightarrow \pi^*]$ transition of A_1 symmetry with a significant double-excitation nature is lower in energy than the corresponding $[\pi \rightarrow \pi^*]$ B_2 transition. In pyrrol the low energy spectrum is dominated by Rydberg states, with a rather isolated S_1 state of A_2 symmetry. Furan has the same type of S_1 state but rather close are $[\pi \rightarrow \pi^*]$ states of B_2 and A_1 symmetry. The question of the excited state geometries has been addressed for furan and pyrrole in high level calculations [47–49], but for the other molecules we could not find data of equivalent quality.

Using symmetry restrictions it was possible to determine the vertical excitation and excited state geometry for pyrrole and furan in the Rydberg and $[\pi \rightarrow \pi^*]$ state with the ROSS/ROKS methods. In Tables 7, 8, 9 and 10, the geometries of the 5-ring molecules in the B_2 $[\pi \rightarrow \pi^*]$ excited state are presented. Upon excitation, they all show a change in the alternation of the single/double bond nature of carbon-carbon distances. The B_2 state optimized in pyrrole is not the first excited state of this symmetry in the vertical excitation but the second and first with $[\pi \rightarrow \pi^*]$ character. This is in contrast to other studies [39,25] where there was another state found slightly lower of this character. Therefore this state was not optimized in the study by Burcl

Table 7
Geometries of the first excited B_2 $[\pi \rightarrow \pi^*]$ state of cyclo-pentadiene (C_{2v} symmetry); the same notation as in table 3 is used. [a] ROSS and ROKS have minima for both, planar and non planar geometries, with the non-planar slightly higher in energy. The optimized CIS geometry has C_s symmetry with an out–of–plane angle for the $C1$ carbon of 29.9 degrees.

	CIS	ROSS	ROKS	TDDFT
r_{C1C2}	1.497	1.473	1.507	1.490
r_{C2C4}	1.412	1.431	1.447	1.444
r_{C4C5}	1.386	1.398	1.382	1.398
r_{C1H}	1.081/1.107	1.163	1.121	1.148
r_{C2H}	1.074	1.085	1.083	1.088
r_{C4H}	1.072	1.082	1.082	1.084
Δ_{C2C1C3}	96.1	100.4	100.5	99.9
Δ_{C1C2C4}	109.4	112.2	110.8	112.2
Δ_{C2C4C5}	107.3	107.6	108.9	107.8
Δ_{H6C1H7}	108.1	96.0	101.9	98.5
Δ_{C2C1H6}	115.1/111.1	115.4	113.7	114.8
Δ_{C1C2H}	124.6	124.1	124.4	124.1
Δ_{C2C4H}	125.7	125.7	124.9	125.1

et al. [25].

Cyclo-pentadiene preserves the C_{2v} symmetry of the molecule also in the excited state, except for the CIS method in which the CH_2 group bends out of plane. The ROKS/ROSS excited state potentials also possess minima for the non-planar geometry which are only slightly higher in energy than the global minima, but have very different emission spectra. This out-of-plane distortion has been recognized in earlier theoretical work to be due to the ionic nature of the singlet state and does not occur in the corresponding triplet state. The other molecules become non-planar and have C_s symmetry in the $[\pi \rightarrow \pi^*]$ state. The coupled-cluster calculations of pyrrole in the literature [47] also did not consider the B_2 $[\pi \rightarrow \pi^*]$ valence transition, but the CASPT2 calculations [49] which were performed within C_{2v} symmetry showed three imaginary frequencies upon analysis of the Hessian.

Results for the B_2 $[\pi \rightarrow \pi^*]$ state of furan are shown in table 9. ROKS and TDDFT are in close agreement for the bond length, the ROSS methods results in shorter bonds close to the oxygen. The oxygen carbon bond is considerably shorter in the CIS calculation. All method show an out–of–plane angle for the

Table 8
Geometries of the first B_2 [$\pi \rightarrow \pi^*$] excited state of thiophene (C_s symmetry); the same notation as in table 3 is used.

	CIS	ROSS	ROKS	TDDFT
r_{SC2}	1.749	1.753	1.765	1.783
r_{C2C4}	1.426	1.452	1.463	1.455
r_{C4C5}	1.365	1.378	1.365	1.382
r_{C2H}	1.075	1.094	1.089	1.095
r_{C4H}	1.073	1.085	1.085	1.087
Δ_{CSC}	86.9	88.7	89.2	87.2
Δ_{SCC}	111.1	110.3	110.6	111.2
Δ_{C2C4C5}	111.4	111.7	112.4	111.7
Δ_{SCH}	122.2	120.9	120.5	120.1
Δ_{C2C4H}	122.9	122.8	122.3	122.5
τ_{SCC}	25.3	24.2	19.6	23.4

Table 9
Geometries of the B_2 [$\pi \rightarrow \pi^*$] excited singlet state of furan (C_s symmetry); the same notation as in table 3 is used. In the ROKS and ROSS methods, the valence excitation is the lower in energy than the correct first excited state which is of Rydberg type.

	CIS	ROSS	ROKS	TDDFT
r_{OC2}	1.355	1.397	1.425	1.420
r_{C2C4}	1.414	1.419	1.452	1.446
r_{C4C5}	1.370	1.390	1.368	1.388
r_{C2H}	1.069	1.106	1.091	1.096
r_{C4H}	1.069	1.084	1.081	1.084
Δ_{COC}	102.2	102.5	103.5	99.5
Δ_{OCC}	110.3	110.6	109.5	110.7
Δ_{CCC}	105.2	106.2	107.4	105.7
Δ_{OCH}	117.4	116.5	115.6	116.1
Δ_{C2C4H}	125.5	125.3	124.5	125.2
τ_{OCC}	24.9	19.0	15.0	25.8

Table 10
Geometries of the B_2 [$\pi \rightarrow \pi^*$] excited singlet state of pyrrole (C_s symmetry); the same notation as in table 3 is used. [a] CASPT2 structure optimized in C_{2v} symmetry; from private communications with B. Roos [49].

	CIS	ROSS	ROKS	CASPT2[a]
r_{NC2}	1.366	1.435	1.436	1.438
r_{NH}	0.990	1.017	1.017	1.001
r_{C2C4}	1.435	1.426	1.460	1.450
r_{C4C5}	1.355	1.370	1.368	1.385
r_{C2H}	1.068	1.081	1.093	1.077
r_{C4H}	1.068	1.084	1.083	1.076
Δ_{CNC}	109.4	104.0	104.0	-
Δ_{NC2C4}	107.5	109.2	107.0	-
Δ_{C2C4C5}	107.7	109.2	107.9	-
Δ_{C2NH}	125.3	115.7	117.9	-
Δ_{NC2H}	122.5	121.0	120.7	-
Δ_{C2C4H}	124.2	124.0	124.5	-

oxygen of about 20 degrees with ROKS having the smallest angle. For the same state in pyrrole, see table 10, ROKS and ROSS results are in close agreement. Within TDDFT and the localized basis set treatment this state was not stable. However, there are results from a CASPT2 calculation within C_{2v} symmetry. These calculations agree very well with the ROSS/ROKS results. Especially the amount of elongation of the carbon nitrogen bond is the same for these methods, a feature missed by the CIS calculation.

In tables 11 and 12 the geometries for the Rydberg [$\pi \rightarrow 3s$] transitions from the ROKS/ROSS and TDDFT calculations are shown to be in close agreement. For pyrrole coparison to CASPT2 [49] and coupled-cluster calculations [47] can be made and we see that the DFT methods give an excellent description of these states. It seems that the asymptotic correction needed for accurate excitation energies is of minor importance for the excited states geometries. This is in agreement with the findings of others [25]. Rydberg state geometries of furan and pyrrole are very sensitive to the basis set used. With the triple-zeta basis set used in calculations for the other molecules, the N-H bond in pyrrole breaks within TDDFT and the molecule dissociates. Adding difuse functions to the basis made the molecule also stable within TDDFT (See Table 12). This process has previously been studied with CASPT2 [50,51]. It has been shown that a small barrier for dissociation of the hydrogen atom indeed exists. In an attempt to further examine the basis set dependence, we

Table 11
Geometries of the A_2 [$\pi \rightarrow 3s$] excited singlet state of furan (C_{2v} symmetry); the same notation as in table 3 is used. [a] TDDFT results from Reference [25].

	CIS	ROSS	ROKS	TDDFT	TDDFT[a]
r_{OC2}	1.321	1.373	1.373	1.376	1.346
r_{C2C4}	1.395	1.410	1.410	1.403	1.405
r_{C4C5}	1.374	1.382	1.382	1.381	1.380
r_{C2H}	1.066	1.087	1.087	1.093	1.080
r_{C4H}	1.068	1.092	1.093	1.112	1.081
Δ_{COC}	107.1	104.9	104.8	104.6	106.0
Δ_{OCC}	110.8	111.2	111.2	111.2	111.0
Δ_{OCH}	117.3	115.9	115.9	115.9	116.6
Δ_{C2C4H}	125.3	125.4	125.4	126.0	125.3

used an priliminary implimentation of the TDDFT method into the plane wave code to calculate the S_1 potential along the N-H bond dissociation coordinate at the fixed C_{2v} ground state ROKS and TDDFT (from the Gaussian based calculations) geometries, respectively. At the ground state geometry a small barrier for dissociation exists in TDDFT, but not at the ROKS (and TDDFT) excited state geometries. A possible explanation for this artifact in the TDDFT method is that the state is largely a charge-transfer excitation, which is known to be difficult to describe with TDDFT. The vertical excitation causes a change in the molecular dipole moment from 1.8 D to -7.8 D.

5.3 Orbital-mixing ROSS/ROKS in absence of symmetry restrictions

Ristricted open–shell methods require the partially occupied orbitals to fullfil symmetry restrictions [57,14]. For the simple case of an open–shell singlet the two singly occupied orbitals have to be in different irreducible representations. These restrictions make it in principle impossible to calculate certain excitations and especially would lead to a complete failure of the method for non symmetric cases. In density functional theory the source of the symmetry restriction may be traced back to the relaxation of the constraint of the expansion coefficients for the determinants. In ensemble density functional theory [58] the coefficients have to be positive and thereby ensure a variational principal. This constraint is relaxed in the ROKS method and a variational energy expression is only recovered together with the symmetry restriction of the orbitals. However, it is found that the symmetry restriction is a sufficient but not always necessary constraint. In earlier applications the ROKS method was successfully applied within molecular dynamics simulations. In

Table 12
Geometries of the A_2 [$\pi \rightarrow 3s$] excited singlet state of pyrrole (C_{2v} symmetry); the same notation as in table 3 is used. [a] from Reference [25]. [b] from Reference [47]. [c] private communications from B.O. Roos [49].

	CIS	ROSS	ROKS	TDDFT[a]	CCSD[b]	CASPT2[c]
r_{NC2}	1.330	1.359	1.359	1.346	1.351	1.351
r_{NH}	1.008	1.075	1.076	1.059	1.049	1.058
r_{C2C4}	1.427	1.439	1.439	1.433	1.448	1.440
r_{C4C5}	1.357	1.375	1.375	1.372	-	1.375
r_{C2H}	1.068	1.089	1.090	1.082	1.089	1.080
r_{C4H}	1.069	1.086	1.087	1.079	1.087	1.076
Δ_{CNC}	110.0	108.9	108.9	109.1	-	-
Δ_{NCC}	108.3	108.7	108.7	108.8	108.4	-
Δ_{NCH}	121.5	120.5	120.5	120.7	120.7	-
Δ_{C2C4H}	124.7	125.2	125.2	125.1	124.9	-

cases where the symmetry constraint is needed the lowest energy solution without the constraint is found to have singly occupied orbitals of mixed symmetry. A rotation of the orbital-space of the two SOMOs occurs (see figure 1) and this mixing lowers the ROKS energy by artificially making the singlet-triplet state splitting vanish. The mixing of the SOMOs results in a drastic and artificial reduction of excitation energies in particular for the [$\pi \rightarrow \pi^*$] excitations in the five-member ring molecules. For s-tetrazine, the mixing of the SOMOs occurs in the [$\pi \rightarrow \pi^*$] state, but it has only a negligible effect on the excited state potential surface.

As a tool for analyzing the mixing, we present the ROKS energy, for a given set of optimized orbitals, as a function of the mixing angle of the two SOMOs in Figure 2. For the B_2 [$\pi \rightarrow \pi^*$] excitations in all five-member rings, the ROKS states of pure symmetry are instable with respect to mixing of the SOMOs, since they correspond to maxima along the dimension of the mixing angle. The effect is even more pronounced for the optimized mixed SOMOs. In the A_2 [$\pi \rightarrow 3s$] Rydberg excitations (and the [$n \rightarrow \pi^*$] excitation in formaldehyde), the ROKS state SOMOs of pure symmetry are local minima along the mixing angle. The minimum for the A_2 [$\pi \rightarrow 3s$] Rydberg excitations are almost identical for ROSS and ROKS, but ROSS has a larger amplitude in the energy-dependence on the mixing angle both for the [$\pi \rightarrow 3s$] and the [$\pi \rightarrow \pi^*$] transitions. The [$n \rightarrow \pi^*$] excitation in s-tetrazine is a borderline case, for which the ROKS method results in a local minimum for the SOMOs of pure symmetry, but not in ROSS.

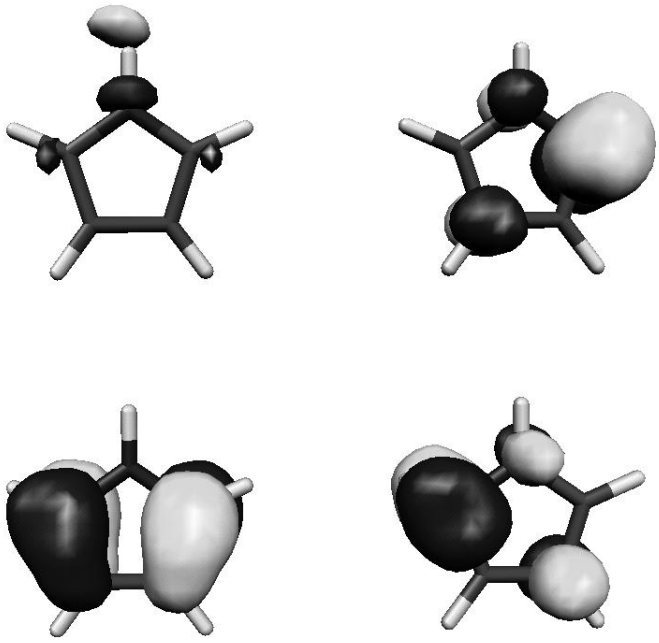

Fig. 1. Vertical excitations of pyrrole with the ROKS calculations. (Left) The SOMOs of the A_2 [$\pi \rightarrow 3s$] Rydberg state, which have the character of the HOMO and LUMO ground state orbitals involved in the excitation. (Right) The de-localized SOMOs B_2 [$\pi \rightarrow \pi^*$] valence state, which can approximately be described as the symmetric and antisymmetric combination of the ground state valence orbitals.

6 Discussion

There is no difference between ROSS and ROKS for the Rydberg excitations. Both methods predict excitation energies too low as is TDDFT. This problem was identified as being connected to the asymptotic limit of current exchange and correlation functionals [59]. However, excited state geometries of Rydberg states are not affected by this shortcomming. Good agreement for the Rydberg state geometries in furan and pyrrole was achieved with ROSS/ROKS and TDDFT. For the [$n \rightarrow \pi^*$] transitions in formaldehyde, s-tetrazine, and pyridine the ROSS method gave higher excitation energies that are closer to experiment than the ROKS method. Geometries for these states agree well with high level calculations (CASPT2, EOM-CCSD) both for ROSS/ROKS and TDDFT. Large differences in excitation energies are found for [$\pi \rightarrow \pi^*$] states. Whereas ROKS predicts vertical excitation energies typically about one eV too low, ROSS energies are too high compared to experiment. Optimized geometries for the [$\pi \rightarrow \pi^*$] states are in qualitative agreement between ROSS, ROKS and TDDFT, but in general larger differences are found than for the other types of excitations. In conclusion, we see that both the ROKS/ROSS and TDDFT methods can give a qualitatively correct description of the excited state potentials. However, none of the methods is generally applicable,

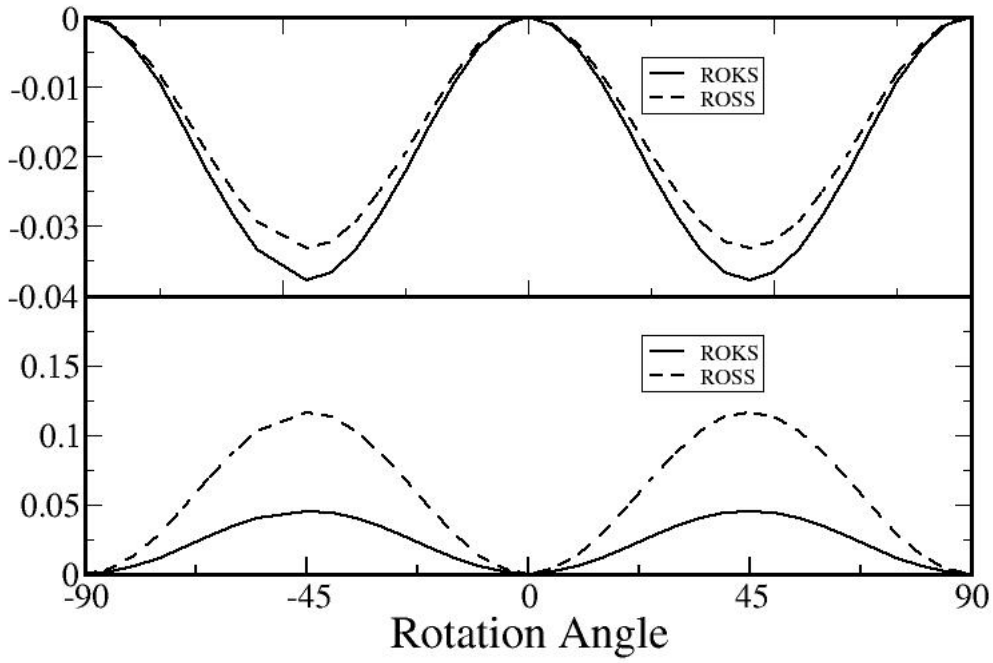

Fig. 2. Dependence of the energy of cyclo-pentadiene (upper panel) and formaldehyde (lower panel) on the mixing angle between the SOMOs in the ROSS/ROKS calculations. The orbitals for the B_2 $[\pi \rightarrow \pi^*]$ excitation (cyclo-pentadiene) and the A_2 $[n \rightarrow \pi^*]$ excitation (formaldehyde) obtained with ROKS[solid line] and ROSS[dashed line] methods.

and the accuracy strongly depends on the nature of the excitation.

In the ROKS and ROSS methods, we noted that without imposing a symmetry constraint a minimum energy is reached with singly occupied orbitals that is not necessarily conform to the symmetry of the molecule. This has been observed previously [14,15] and termed delocalization. This need for a symmetry constraint and the problems with excited state ordering for close-lying excitations restrict the applicability of the restricted open–shell methods. Especially, for $[\pi \rightarrow \pi^*]$ transitions the development of a simple method that could replace the symmetry constraints in the open-shell methods would be desirable. However, when they are applicable, e.g. for isolated $[n \rightarrow \pi^*]$ states, the high accuracy of the restricted open-shell methods seen in this comparative study, is a very promising result for the study of photo-chemical processes in complex systems. In particular, the explicit inclusion of a crystal surrounding or solvent around the chromophore will make it possible to create a highly realistic model of many experimental situations.

References

[1] R. Car and M. Parrinello, Phys. Rev. Lett., **55**, 2471, (1985).

[2] D. Marx and J. Hutter, Ab initio molecular dynamics: Theory and implementation, in Modern Methods and Algorithms of Quantum Chemistry, J. Grotendorst (Ed.), Forschungszentrum Jülich, NIC Series, Vol. 1, (2000)

[3] M. Parrinello, Solid State Comm., **102**, 107, (1997).

[4] A.H. Zewail, J. Phys. Chem. A, **104**, 5660, (2000).

[5] P.E.M. Siegbahn, *The configuration interaction method*, in Lecture Notes in Chemistry: European Summer School in Quantum Chemistry (Springer-Verlag, Berlin, 1992) vol. 58

[6] K. Andersson, P.-Å. Malmqvist, B.O. Roos, A.J. Sadlej, and K. Wolinski, J. Phys. Chem., **94**, 5483, (1990).

[7] K. Andersson, P.-Å. Malmqvist, and B.O. Roos, J. Chem. Phys., **96**, 1218, (1992).

[8] T. Crawford and H. Schaefer, in "Reviews in Computational Chemistry", Vol. 14, Eds. K.B. Lipkowitz and D. B. Boyd, Wiley-VCH, 1999.

[9] I. Frank, J. Hutter, D. Marx, and M. Parrinello, J. Chem. Phys., **108**, 4060, (1998).

[10] C. Molteni, I. Frank, and M. Parrinello, J. Am. Chem. Soc., **121**, 12177, (1999).

[11] C. Molteni, I. Frank, and M. Parrinello, Comp. Mat. Sci., **20**, 311, (2001).

[12] N.L. Doltsinis and D. Marx, Phys. Rev. Lett. **88**: art. no. 166402 (2002).

[13] M. Filatov and S. Shaik, Chem. Phys. Lett., **288**, 689, (1998).

[14] M. Filatov and S. Shaik, J. Chem. Phys., **110**, 116, (1999).

[15] J. Gräfenstein, E. Kraka, and D. Cremer, Chem. Phys. Lett., **288**, 593, (1998).

[16] J. Gräfenstein and D. Cremer, Phys. Chem. Chem. Phys., **2**, 2091, (2000).

[17] M.E. Casida, in "Recent Developments and Applications of Modern Density Functional Theory, Theoretical and Computational Chemistry", Vol. 4, Ed. J.M. Seminario, Elsevier, Amsterdam, 1996

[18] R.E. Stratmann and G.E. Scuseria, J. Chem. Phys., **109**, 8218, (1998).

[19] M.E. Casida, in "Recent Advances in Density Functional Methods", Vol. 1 Ed. D.P. Chong, World Scientific, Singapore, 1995

[20] T. Ziegler, A. Rauk, and E.J. Baerends, Theor. Chim. Acta, **43**, 261, (1977).

[21] T. Ziegler, Chem. Rev., **91**, 651, (1991).

[22] C. van Caillie and R.D. Amos, Chem. Phys. Lett., **308**, 249, (1999).

[23] C. van Caillie and R.D. Amos, Chem. Phys. Lett., **317**, 159, (2000).

[24] M.E. Casida, K.C. Casida, and D.R. Salahub, Int. J. Quantum Chem., **70**, 933, (1998).

[25] R. Burcl, R.D. Amos, and N.C. Handy, Chem. Phys. Lett., **355**, 8, (2002).

[26] M. Head-Gordon, M. Oumi, and D. Maurice, Mol. Phys., **96**, 593, (1999).

[27] The calculations have been performed with the code CPMD version 3.5, written by Jürg Hutter et al., Copyright IBM Corp 1990-2001, Copyright MPI für Festkörperforschung Stuttgart 1997-2001.

[28] L. Kleinman and D.M. Bylander, Phys. Rev. Lett. **48**, 1425, (1982).

[29] P. Giannozzi (1993), unpublished.

[30] N. Troullier and J.L. Martins, Phys. Rev. B, **43**, 1993, (1991).

[31] A.D. Becke, Phys. Rev. A, **38**, 3098, (1988).

[32] C. Lee, W. Yang, and R.G. Parr, Phys. Rev. B, **37**, 785, (1988).

[33] G.J. Martyna and M.E. Tuckerman, J. Chem. Phys., **110**, 2810, (1999).

[34] D. Laikov, unpublished

[35] A. Schäfer, C. Huber, and R. Ahlrichs, J. Chem. Phys., **100**, 5829, (1994).

[36] K. Eichkorn, F. Weigend, O. Treutler, and R. Ahlrichs, Theor. Chim. Acta, **97**, 119, (1977).

[37] D.N. Laikov, Chem. Phys. Lett., **281**, 151, (1997).

[38] R. Bauernschmitt, M. Häser, O. Treutler, and R. Ahlrichs, Chem. Phys. Lett., **264**, 573, (1997).

[39] D.J. Tozer, R.D. Amos, N.C. Handy, B.O. Roos,and L. Serrano-Andrés, Mol. Phys., **97**, 859, (1999).

[40] Chr. Møller and M.S. Plesset, Phys. Rev., 618, (1934).

[41] Gaussian 98, Revision A.7, M. J. Frisch, G. W. Trucks, H. B. Schlegel, G. E. Scuseria, M. A. Robb, J. R. Cheeseman, V. G. Zakrzewski, J. A. Montgomery, Jr., R. E. Stratmann, J. C. Burant, S. Dapprich, J. M. Millam, A. D. Daniels, K. N. Kudin, M. C. Strain, O. Farkas, J. Tomasi, V. Barone, M. Cossi, R. Cammi, B. Mennucci, C. Pomelli, C. Adamo, S. Clifford, J. Ochterski, G. A. Petersson, P. Y. Ayala, Q. Cui, K. Morokuma, D. K. Malick, A. D. Rabuck, K. Raghavachari, J. B. Foresman, J. Cioslowski, J. V. Ortiz, A. G. Baboul, B. B. Stefanov, G. Liu, A. Liashenko, P. Piskorz, I. Komaromi, R. Gomperts, R. L. Martin, D. J. Fox, T. Keith, M. A. Al-Laham, C. Y. Peng, A. Nanayakkara, C. Gonzalez, M. Challacombe, P. M. W. Gill, B. Johnson, W. Chen, M. W. Wong, J. L. Andres, C. Gonzalez, M. Head-Gordon, E. S. Replogle, and J. A. Pople, Gaussian, Inc., Pittsburgh PA, 1998.

[42] N.L. Doltsinis and M. Sprik, Chem. Phys. Lett., **330**, 563, (2000).

[43] R. Bauernschmitt and R. Ahlrichs, Chem. Phys. Lett., **256**, 454, (1996).

[44] Z.L. Cai and J.R. Reimers, J. Phys. Chem. A, **104**, 8389, (2000).

[45] P.J. Stephens, F.J. Devlin, C.F. Chabalowski,and M.J. Frisch, J. Chem. Phys., **98**, 11623, (1994).

[46] M. Schütz, J. Hutter, and P. Lüthi, J. Chem. Phys., **103**, 7084, (1995).

[47] O. Christiansen, J. Gauss, J.F. Stanton,and P. Jørgenssen, J. Chem. Phys., **111**, 525, (1999).

[48] O. Christiansen and P. Jørgenssen, J. Am. Chem. Soc., **120**, 3423, (1998).

[49] B.O. Roos, private communication

[50] A.L. Sobolewski and W. Domcke, Chem. Phys., **259**, 181, (2000).

[51] A.L. Sobolewski and W. Domcke, Chem. Phys. Lett., **321**, 479, (2000).

[52] M. Merchan and B.O. Roos, Theor. Chim. Acta, **92**, 227, (1995).

[53] A.C. Scheiner and H.F. Schaefer III, J. Chem. Phys. **87**, 3539, (1987).

[54] M. Nooijen, J. Phys. Chem. A, **104**, 4553, (2000).

[55] C. Adamo and V. Barone, Chem. Phys. Lett., **330**, 152, (2000).

[56] MOLCAS Version 5. Kerstin Andersson, Maria Barysz, Anders Bernhardsson, Margareta R.A. Blomberg, D. L. Cooper, Timo Fleig, Markus P. Fülscher, Coen de Graaf, Bernd A. Hess, Gunnar Karlström, Roland Lindh, Per-Åke Malmqvist, Pavel Neogrády, Jeppe Olsen, Björn O. Roos, Andrzej J. Sadlej, Martin Schütz, Bernd Schimmelpfennig, Luis Seijo, Luis Serrano-Andrés, Per E.M. Siegbahn, Jonna Stålring, Thorstein Thorsteinsson, Valera Veryazov and Per-Olof Widmark, Lund University, Sweden (2000).

[57] C.C.J. Roothaan, Rev. Mod. Phys., **32**, 179 (1960).

[58] A.K. Theophilou, J. Phys. C, **12**, 5419, (1979).

[59] D.J. Tozer and N.C. Handy, J. Chem. Phys., **109**, 10180, (1998).